

Transmission studies of left-handed materials

P. Markoš^{*} and C. M. Soukoulis

Ames Laboratory and Department of Physics and Astronomy, Iowa State University, Ames, Iowa 50011

(Received 31 August 2001; published 7 December 2001)

Left-handed materials are studied numerically using an improved version of the transfer-matrix method. The transmission, reflection, phase of reflection, and absorption are calculated and compared with experiments for both single split-ring resonators with negative permeability and left-handed materials, which have both the permittivity ϵ and permeability μ negative. Our results suggest ways of positively identifying materials that have both ϵ and μ negative, from materials that have either μ or ϵ negative.

DOI: 10.1103/PhysRevB.65.033401

PACS number(s): 73.20.Mf, 41.20.Jb, 42.70.Qs

Photonic band gap (PBG) structures were originally introduced to control the electromagnetic wave propagation of matter.^{1,2} Not only dielectric^{1,2} but metallic structures³⁻⁵ were proposed for applications in the microwave and infrared regions. Very recently, a new area of research, called left-handed materials (LHMs), has been introduced by Pendry *et al.*^{6,7} and Smith *et al.*⁸ LHMs are by definition composites, whose properties are not determined by the fundamental physical properties of their constituents but by the shape and distribution of specific patterns included in them. Thus, for certain patterns and distribution, the measured effective permittivity ϵ_{eff} and the effective permeability μ_{eff} can be made to be less than zero. In such materials, the phase and group velocity of an electromagnetic wave propagate in opposite directions giving rise to a number of novel properties.⁹ This behavior has been called “left-handedness,” a term first used by Veselago¹⁰ over 30 years ago, to describe the fact that the electric field, magnetic intensity and propagation vector are related by a left-handed rule.

By combining a two-dimensional (2D) array of split-ring resonators (SRRs) with a 2D array of wires, Smith *et al.*⁸ demonstrated for the first time the existence of left-handed materials. Pendry *et al.*⁷ has suggested that an array of SRRs give an effective μ_{eff} , which can be negative close to its resonance frequency. It is also well known^{3,6} that an array of metallic wires behaves like a high-pass filter, which means that the effective dielectric constant is negative at low frequencies. Very recently, Shelby *et al.*¹¹ demonstrated experimentally that the index of refraction n is negative for a LHM. Also, Pendry¹² has suggested that a LHM with negative n can make a perfect lens.

In this paper, we present systematic numerical results for the transmission, reflection and absorption properties of left-handed materials. An improved version of the transfer-matrix method¹³ (TMM) is used. Qualitative agreement with experiments^{8,14} is obtained, and new predictions about the absorption and the phase of the reflection, to be checked experimentally, are presented.

The transfer-matrix method¹³ is used to calculate the EM transmission and reflection of LHMs. In the TMM, we assume that the sample is connected with two semi-infinite leads (with $\epsilon = \mu = 1$). The incident wave (say, from the right) is either reflected or transmitted through the sample. Then, the transfer matrix is defined by relating the incident fields on one side of the structure with the outgoing fields¹⁵

$$\mathcal{T} = \begin{pmatrix} t_-^{-1} & -t_-^{-1}r_- \\ r_+t_-^{-1} & t_+ - r_+t_-^{-1}r_- \end{pmatrix}. \quad (1)$$

Here t_- (t_+) is the transmission matrix for the wave incident from the right (left) of the slab and r_- (r_+) are corresponding reflection matrices.

In numerical calculations, the total volume of the system is divided into small cells and fields in each cell are coupled to those in the neighboring cell. We assume periodic boundary conditions in the directions parallel to the interfaces. In the leads, the transfer matrix can be diagonalized analytically. If the number of mesh points in the plane perpendicular to the propagation is N , then the transfer matrix is of the size $4N \times 4N$. One half of the eigenvectors corresponds to the propagation to the left, and the second half to the right. Corresponding transmission and reflection matrices t and r are then of the size $2N \times 2N$. Factor 2 is due to polarization. Using the general form of the transfer matrix as given by Eq. (1) we express the transmission matrix explicitly as

$$t_-^{-1} = LTR \quad (2)$$

where L and R are matrices $4N \times 2N$ ($2N \times 4N$) that contains the left (right) eigenvectors of left-going wave. For the frequency range of interest, transfer matrix has only one propagating mode for each direction. We find then the transmission coefficient as

$$T_{ij} = \sum_{k=1}^{2N} t_{ik} t_{jk}^\dagger \quad (3)$$

with $i, j = 1$ or 2 for the p or s polarized wave. The TMM has been previously¹ applied in studies of metallic structures,^{3-5,16} as well as in dielectric structures. In all these examples, the agreement between theoretical predictions and experimental measurements was very good.¹

Following the algorithm described by Pendry *et al.*,¹⁷ we have developed a new version of the transfer-matrix code. The main change from the standard algorithm commonly used in the PBG studies¹³ is the faster normalization of the transmitted waves in the calculation of the transmission coefficient through the structure.¹⁸

The TMM has been used to simulate the reflection and transmission from an array of square SRRs. Figure 1(a) shows a diagram of a single square SRR of the type used for

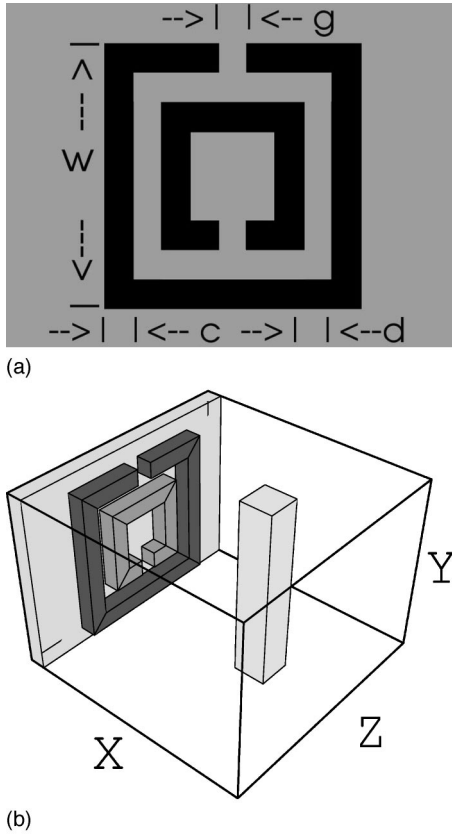


FIG. 1. (a) The SRR consists from two splitted metallic rings located on a dielectric board. We approximate the rings by squares of size w . Other parameters, which influence the resonance frequency ν_0 , are the ring width c , the radial gap d , and the azimuthal gap g . (b) Configuration of the unit cell of a LHM. EM wave propagates along the z axis and the magnetic intensity is parallel to the SRR axis, which is the x axis. We assume periodic boundary conditions in the x and y directions. In the numerical simulations the unit cell is $5 \times 3.63 \times 5$ mm and is divided to $N_x \times N_y \times N_z = 15 \times 11 \times 15$ small cells. This defines the length unit = 0.33 mm. The number of unit cells in z direction varies from 6 to 20, and is 9 for most of the cases presented here.

our simulations and for experiments.¹⁵ In our case we have $c = d = g = 0.33$ mm and the size of SRR $w = 3$ mm. Figure 1(b) shows a three-dimensional realization of the actual LHM that we have simulated.

Figure 2 presents the results of the transmission versus frequency for the split ring resonators alone, and of the LHM, which consists of the SRRs with metallic wires placed uniformly between the SRRs. The square array of metal wires alone behaves as a high pass filter with a cutoff frequency $\nu_c = 19$ GHz. The cutoff frequency ν_c of the metallic wires is given by $\nu_c = c_{\text{light}} / 2a \sqrt{\epsilon_0}$, where a is the distance between the wires, c_{light} is the velocity of light in the air, and ϵ_0 is the dielectric constant of the background. In our case $a = 5$ mm and $\epsilon_0 = 1$. The cutoff frequency is independent of either value of $\text{Re } \epsilon_m$ or $\text{Im } \epsilon_m$ of the metal, provided that either $|\text{Re } \epsilon_m| > 1000$ or $|\text{Im } \epsilon_m| > 1000$. The dot-dashed curve is that of the SRR array with $a = 5$ mm. By adding wires uniformly between the SRRs, a pass band occurs where both

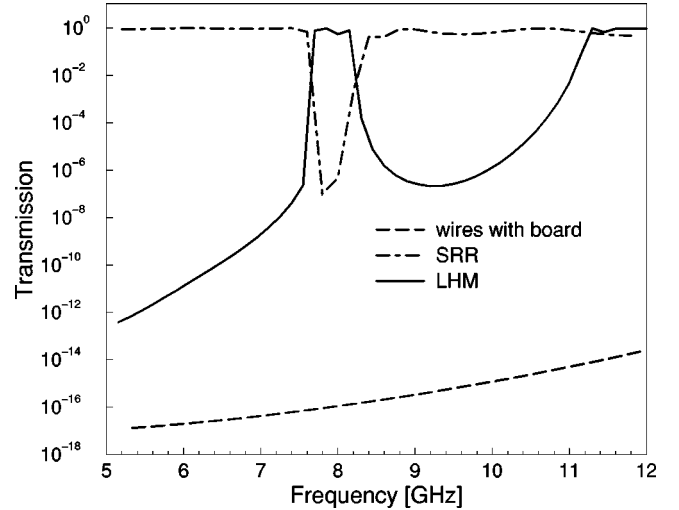


FIG. 2. Transmission of electromagnetic waves through arrays of SRRs, wires and through a LHM with a real permittivity for the metal $\epsilon_m = -3000$. The dielectric constant of the board is $\epsilon_b = 3.4$. The thickness of the wire is 1×1 mm. Magnetic intensity is parallel to the SRR axis. For the other polarization, no resonant gap was observed.

μ_{eff} and ϵ_{eff} are negative (solid line). The transmitted power of the LHM is very high (close to one), because no $\text{Im } \epsilon_m$ is taken for the metal. We also studied more realistic cases with nonzero $\text{Im } \epsilon_m$. We found that the resonance frequency ν_0 increases as $|\epsilon_m|$ increases and saturates to a value of $\nu_0 \approx 8.5$ as $|\epsilon_m| \rightarrow \infty$. This is clearly shown in Fig. 3 where we plot ν_0 versus the magnitude of $\epsilon_m = \epsilon_r + i\epsilon_i$. The resonance frequency is also sensitive to the permittivity of the board that the SRR is lying and of the embedding medium. We have found that ν_0 drops as the dielectric constant of the embed-

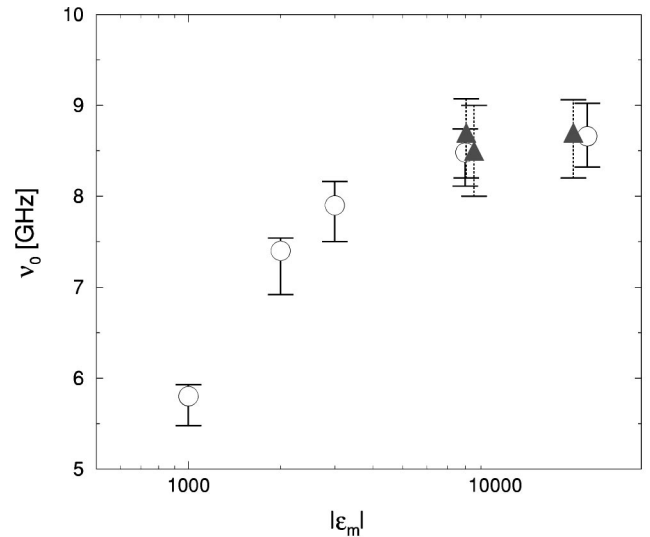


FIG. 3. Dependence of the resonance frequency ν_0 on the absolute value of the permittivity $|\epsilon_m|$ of metallic compounds. Both real (open circles) and complex (solid triangles) values of permittivity were considered. Error bars indicate the width of gap. ν_0 does not depend on ϵ for $|\epsilon| \geq 10^4$.

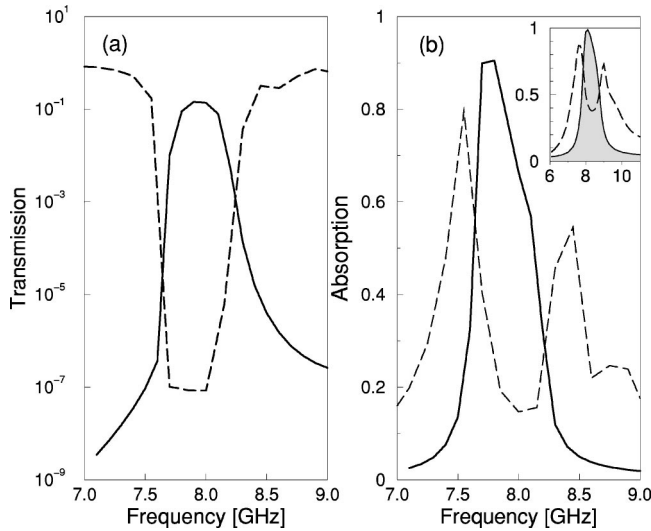


FIG. 4. (a) Transmission through arrays of SRRs (dashed line) and through a LHM (solid line) with a complex permittivity for the metal. (b) Absorption versus frequency for the same system as shown in (a). Permittivity of metal is $\epsilon = -3000 + i 100$. Insert shows absorption in a composite system with a frequency dependent ϵ_{eff} and μ_{eff} given by Eqs. (4) and (5).

ding media ϵ_a increases. ν_0 drops from its value of 8 GHz for $\epsilon_a = 1$ to a value of 6 GHz when $\epsilon_a = 2.0$. The value ν_0 increases by decreasing the value of the permittivity ϵ_b of the dielectric board. ν_0 increases to a value of 9 GHz from 8 GHz when ϵ_b drops to a value of 1.4 from its original value of $\epsilon_b = 3.4$.

The results presented in Fig. 2 are done by assuming that the permittivity of the metal ϵ_m had a large negative value. As one can see from Fig. 2, the value of the transmission for the LHM is very close to one. This value drops considerable if one uses the fact that ϵ_m for the metal is complex. In Fig. 4(a) we present results similar to that in Fig. 2, with the only difference being the value of the $\text{Im } \epsilon_m$. Notice that the position of the resonance peak is at the same value at around 7.8 GHz. Due to the nonzero $\text{Im } \epsilon_m$ there is considerable drop of the peak of the transmission for the LHM. We have not done a systematic effort to fit the experimental results of Smith *et al.*⁸

In Fig. 4(b), we present new results of the frequency dependence of the absorption for either the SRR or the LHM. For the arrays of SRRs alone, we find that absorption has two peaks, shown as dashed lines in Fig. 4(b), while the LHM has only one absorption peak [shown as a solid line in Fig. 4(b)] at the center of its resonance frequency. This might be a reasonable way of identifying materials that are left-handed and have both their ϵ_{eff} and μ_{eff} negative. On the inset of Fig. 4(b) we present the frequency dependence of the absorption as they were found for a simple model, using^{6,7} the following forms of the frequency dependence of the effective permittivity and permeability:

$$\epsilon_{\text{eff}}(\nu) = 1 - \frac{\nu_p^2}{\nu^2 + i\nu\gamma} \quad (4)$$

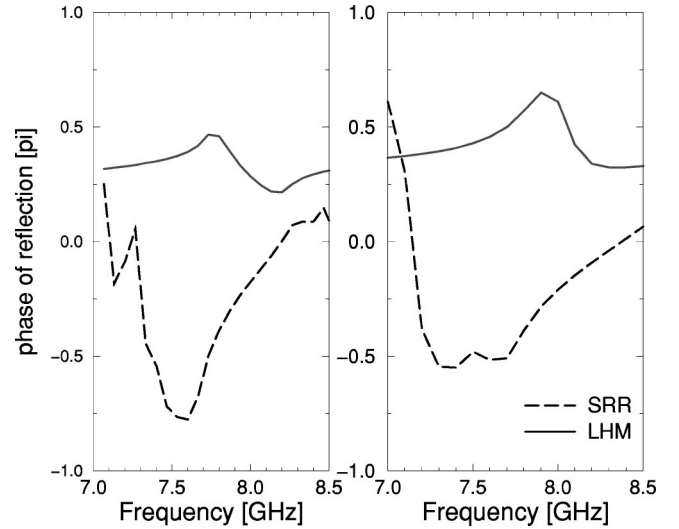


FIG. 5. Left: Phase of reflection for both SRR and LHM. $\epsilon_m = -3000 + i 100$. Right: The same for homogeneous model.

where ν_p is the plasma frequency or cutoff frequency ν_c of the wires, $\nu_c = \nu_p \approx 19$ GHz in our case. A negative μ_{eff} accounts for the deep in the transmission in SRRs and its form^{6,7} is given by

$$\mu_{\text{eff}}(\nu) = 1 - \frac{F\nu^2}{\nu^2 - \nu_0^2 + i\nu\Gamma} \quad (5)$$

where F is the filling factor which is in our case close to 0.3 and $\nu_0 \approx 7.9$ GHz is the resonance frequency of the SRR. We used that $\gamma = \Gamma = 0.2$ GHz. There is very good agreement between the solution of present model and numerical simulations of real structures.

Equations (4) and (5) enable us also to explain the difference between the absorption of SRR and LHM. The portion A of the field absorbed in the system is

$$A = (1 - R)(1 - e^{-\alpha z}) \quad (6)$$

where R is the reflection, α is the absorption coefficient, and z is the length of the system. α is proportional to the imaginary part of the refraction index. Owing to the form of Eqs. (4) and (5), both α and $1 - \exp(-\alpha z)$ possess a sharp maximum near the resonance frequency and are small far outside the resonance gap. This is true both for SRR and LHM. The main difference between the absorption of SRR and LHM is given by the first term in Eq. (6). In SRR, $1 - R$ is close to unity for all frequencies outside the resonance gap, where $1 - R$ is zero. The absorption A , given by the product in Eq. (6), is therefore nonzero only on the borders of the resonance gap where both functions are nonzero.¹⁹ In contrast to SRR, $1 - R$ possess a maximum inside the resonance gap. Then, absorption A should have therefore one maximum as shown in Fig. 4(b).

In Fig. 5 we present the typical results of the phase of the reflection for both the LHM and the array of SRRs. Obtained data are in qualitative agreement with that obtained from the homogeneous model given by Eqs. (4) and (5). Notice that there is a substantial difference in their characteristics. The

phase of reflection increases with frequency in SRR. In a LHM, the phase as a function of frequency possesses two extrema on the two sides of the resonance gap and decreases with the frequency inside the gap. We derived the same behavior of phase from the standard textbook formulas for the reflection,²⁰ if the frequency dependent permittivity and permeability follow relations (4) and (5).

We used an improved transfer-matrix method for numerical studies of complex meta-materials. Our numerical data of transmission confirms the presence of a resonant gap, in agreement with theoretical predictions and experiments. Our method enables us to analyze also the reflection and absorption of the light and also the change of the phase of the reflected field. We compare our numerical data that of a simple homogeneous model defined by effective permittivity and permeability [Eqs. (4), and (5)] and found very good qualitative agreement either with numerical simulations or

with theoretical predictions.²⁰ This supports our belief that for the frequencies in the resonance gap our structure possesses negative effective μ_{eff} and negative effective ϵ_{eff} . Although our method does not allow us to vary the size parameters of SRR continuously, we are able to predict, at least qualitatively, how the position of resonance gap depends on various parameters of the system. We believe that generalization of our numerical method to nonhomogeneous discretization of space will enable us to analyze more realistic structures.

We thank D. R. Smith and I. El-Kady for fruitful discussions. Ames Laboratory is operated for the U.S. Department of Energy by Iowa State University under Contract No. W-7405-Eng-82. This work was supported by the Director of Energy Research, Office of Basic Science, DARPA and NATO Grant No. PST.CLG.978088. P.M. thanks Ames Laboratory for its hospitality and support and Slovak Grant Agency for financial support.

*Permanent address: Institute of Physics, Slovak Academy of Sciences, Dúbravská cesta 9, 842 28 Bratislava, Slovakia.

¹ *Photonic Band Gap Materials*, edited by C.M. Soukoulis (Kluwer, Dordrecht, 1996).

² J.D. Joannopoulos, R.D. Mead, and J.N. Winn, *Photonic Crystal* (Princeton University Press, Princeton, 1995); J.D. Joannopoulos, P.R. Villeneuve, and S. Fan, *Nature* (London) **386**, 143 (1997).

³ D.R. Smith, S. Schultz, N. Kroll, M. Sigalas, K.M. Ho, and C.M. Soukoulis, *Appl. Phys. Lett.* **65**, 645 (1994).

⁴ E. Özbay, B. Temelkuran, M. Sigalas, G. Tuttle, C.M. Soukoulis, and K.M. Ho, *Appl. Phys. Lett.* **69**, 3397 (1996); M. Sigalas, C.T. Chan, K.M. Ho, and C.M. Soukoulis, *Phys. Rev. B* **52**, 11 744 (1995).

⁵ D.F. Sievenpiper, E.H. Yablonovitch, J.N. Winn, S. Fan, P.R. Villeneuve, and J.D. Joannopoulos, *Phys. Rev. Lett.* **80**, 2829 (1998).

⁶ J.B. Pendry, A.J. Holden, W.J. Stewart, and I. Youngs, *Phys. Rev. Lett.* **76**, 4773 (1996); J.B. Pendry, A.J. Holden, D.J. Robbins, and W.J. Stewart, *J. Phys.: Condens. Matter* **10**, 4785 (1998).

⁷ J.B. Pendry, A.J. Holden, D.J. Robbins, and W.J. Stewart, *IEEE Trans. Microwave Theory Tech.* **47**, 2075 (1999).

⁸ D.R. Smith, W.J. Padilla, D.C. Vier, S.C. Nemat-Nasser, and S. Schultz, *Phys. Rev. Lett.* **84**, 4184 (2000); D.R. Smith and N. Kroll, *ibid.* **85**, 2933 (2000).

⁹ J.B. Pendry, *Phys. World* **13**, 27 (2000).

¹⁰ V.G. Veselago, *Usp. Fiz. Nauk* **92**, 517 (1968) [*Sov. Phys. Usp.*

10, 509 (1968)].

¹¹ R.A. Shelby, D.R. Smith, and S. Schultz, *Science* **292**, 77 (2001).

¹² J.B. Pendry, *Phys. Rev. Lett.* **85**, 3966 (2000).

¹³ J.B. Pendry and A. MacKinnon, *Phys. Rev. Lett.* **69**, 2772 (1992); J.B. Pendry, *J. Mod. Opt.* **41**, 209 (1994).

¹⁴ R.A. Shelby, D.R. Smith, S.C. Nemat-Nasser, and S. Schultz, *Appl. Phys. Lett.* **78**, 489 (2001).

¹⁵ J.B. Pendry and P.M. Bell, in *Photonic Band Gap Materials*, Ref. 1 p. 203.

¹⁶ I. El-Kady, M.M. Sigalas, R. Biswas, K.M. Ho, and C.M. Soukoulis, *Phys. Rev. B* **62**, 15 299 (2000).

¹⁷ J.B. Pendry, A. MacKinnon, and P.J. Roberts, *Proc. R. Soc. London, Ser. A* **437**, 67 (1992).

¹⁸ For the structures described in Fig. 1, the typical CPU time necessary to calculate transmission for a given frequency is approximately 55 sec/unit cell on an alpha workstation (533 MHz Alpha 21164 processor with 512 MB memory). Most of the CPU time is spent in the normalization of the actual numerical data. As our structure is highly nonhomogeneous (permittivity of systems varies in three or more orders from site to site), we have to normalize the numerical data after 3–4 steps. For studies of more homogeneous samples, the CPU time could be reduced by a factor of 2 to 5.

¹⁹ For wider resonance gap, the right absorption peak in the SRR may disappear.

²⁰ G.R. Fowles, *Introduction to Modern Optics*, 2nd. ed. (Holt, Rinehart and Winston, New York, 1968), Chap. 6.